Lung segmentation from CT images: Impact of different window settings on the accuracy of segmentation

[1]Manas Jyoti Das,[2*]Lipi B. Mahanta
[1]Research Scholar, Computational and Numerical Sciences, IASST, Guwahati, Assam, India,
[2]Associate Professor, Central Computational and Numerical Sciences, IASST, Guwahati, Assam, India

Abstract :Proper segmentation of the lung region from a computed tomography (CT) image, which consists of other anatomical features, is an essential step in automated diagnosis of various lung diseases. The accuracy at which the segmentation needs to be done is vital, as a small under or over-segmentation can lead to an erroneous diagnosis. It has been shown here that CT image acquisition technique plays a vital role in segmenting the lung region. The segmentation for lung region from images acquired via a mediastinum window setting can produce lung region which are less erroneous than an image acquired via the lung window setting. Thresholding and fuzzy C-means are used for segmentation and comparison is done against a reference set of images. The study is done using internal dataset of CT images collected from NABL (National Accreditation Board for Testing and Calibration) radiological laboratory. It has been found that the $\boldsymbol{F_1}$score of mediastinum window images for lung region is found to be higher than the $\boldsymbol{F_1}$ score of images acquired via lung window. This proves that segmentation accuracy obtained from mediastinum window images is higher than that of lung window.

IndexTerms **- Lung CT; Segmentation; Lung window; Mediastinum window; software induced Mediastinum window; comparison.**

I. INTRODUCTION

Computed tomography (CT) is the most widely used noninvasive technique [11] to capture the details of various anatomical structures of the lung. CT images help in diagnosis of various kind of lung diseases based on many features present in a CT image. Computer aided diagnosis (CAD) systems extract these features and use them in forming decisions [9, 13]. One of the prerequisite of a CAD system is correct segmentation of the lung tissue [12] or lung region. Automatic segmentation is a necessity approach [12], as manual [8] delineation takes more time and is tedious and above all subjective.

Till date automated lung segmentation algorithms [3, 15, 16, 17] used data sets in window setting [7] which are known as lung window. This window setting emphasize the anatomy of the lung and the images so produced by this window contain detailed view of reticular opacity, bronchia structure and disease related features like fibrosis, honeycombing etc. There are different window settings available that give emphasis on different anatomy of the thorax. A different and very commonly used window setting is the Mediastinum Window (MW). This window setting gives emphasis on the mediastinum of the thorax and masks most of the details of the lung region as shown in **Fig-1**.

In this paper, a study on the appropriateness of either of the two windows for superior accuracy of segmentation is presented. Two automatic lung segmentation techniques: iterative thresholding [1, 4, 10] and fuzzy C-means (FCM) [5, 14], are used to segment out the lung part from the respective window settings. Evaluating the performance of a lung segmentation technique is difficult, as the mask of lung region of the reference image is formed out of consensus among different radiologist, so true lung boundary is not known. Thus, the segmentation error that we are reporting is only with respect to the reference image that we have obtained. A reference set of images, as binary mask, are created by the radiologist to evaluate the segmentation accuracy between different window settings. Sorensen-Dice coefficient or F_1score is used to show the accuracy.

Two important concepts for the study are CT image acquisition and Window settings.

CT image acquisition:

The CT scanner acquires raw data, also be termed as 'scan data', from each scan. These raw data are not sectioned into pixels, an essential step for computer processing. Hence these data are transformed into images by a process known as image reconstruction. The reconstructed data consists of Hounsfield values, which determine the pixel values of the images. A single Hounsfield value is assigned to each pixel by a reconstruction algorithm or filter or convolutional filter or kernel. In this paper we will be using the term reconstruction algorithm. The value that a pixel gets is the average of all the Hounsfield value measured for that particular pixel.

There are two [7] kinds of reconstruction techniques. One is called prospective reconstruction: it takes the raw data and creates an image automatically during the scanning process. In the other technique, the raw data is saved and used to generate new images using different reconstruction algorithms. This type of reconstruction is termed as retrospective reconstruction. As raw data contains all the measurements that are being captured by the detector array, a variety of images can be created with the raw data.

There are various reconstruction algorithms, used in prospective reconstruction, focusing on different aspects of anatomy. These algorithms transform the raw data associated with each pixel into a value (Hounsfield unit) that can be represented as an image. The software in the CT scanner provides these algorithms, or filters, to reconstruct an image, depending on requirement. The CT scanner operator chooses a specific algorithm (depending on protocol) on how to filter the raw data. Mediastinum reconstruction algorithms are applied to enhance the thorax (**Fig-1**). Similarly for enhancing the lung, a lung enhancement reconstruction algorithm will be used (**Fig-2**). Bone reconstruction algorithm gives emphasis to those raw data that represent a bone measurement (**Fig-3**).

Fig 1: Image reconstruction using mediastinum enhancement algorithm

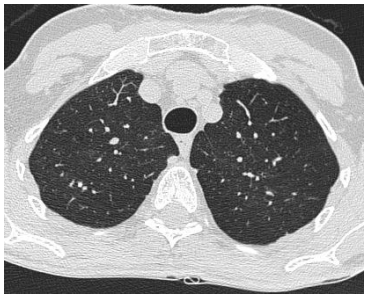

Fig 2: Image Reconstruction using lung enhancement algorithm

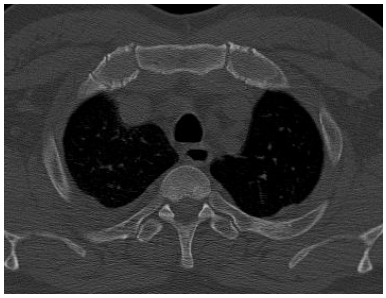

Fig 3: Image reconstruction using bone enhancement algorithm

There are 2000 different Hounsfield values [2, 7], or more, depending on the scanner type. Digital images from the scanner are usually stored as DICOM data structure which usually stores 2000 different Hounsfield values. These values in a DICOM data structure ranges from -1000(air) to +1000(bone). This range may vary depending on scanner type, but these values are representative of most scanners. It is required to manipulate Hounsfield values so as to have an image that either enhances or suppresses certain range of values. To achieve this two concepts are central: one is window width [2, 7] and another is window level [2, 7].

Window settings:

If there are *N* number of Hounsfield values in a certain image and we choose windows width to be *M*, where *N*>*M*, then values higher than the selected range *M* will be white and values lower than the range appears black. So, only *M* number of values will be represented on an image. For a certain windows width the Hounsfield values are grouped together as shown in **Fig-4**.

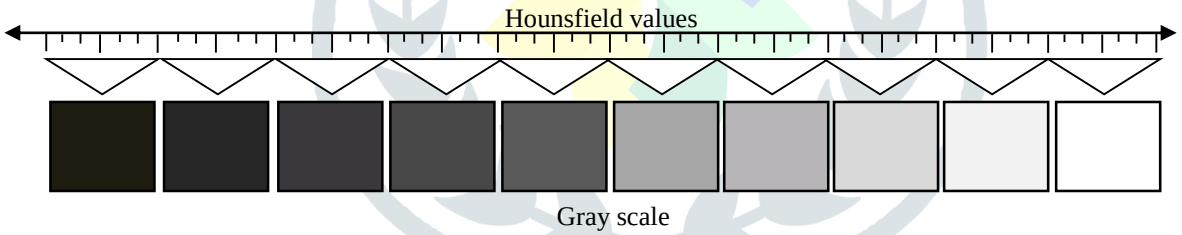

Fig 4: A simplified illustration of 61 Hounsfield values divided into 10 different shades of gray.

The window level *C* is the midpoint of the windows width *M*. If there are n Hounsfield values and *M* be the windows width then *C* is represented as

$$C \geq ceil\left(\frac{M}{2}\right) \quad (1)$$

and

$$n - C < ceil\left(\frac{M}{2}\right) \quad (2)$$

A windows level selects the range of Hounsfield numbers that will be displayed. In other words windows width gives the quantity of values to display and window level gives the range of these quantities from a centre *C*.

Mediastinum Window (MW) or soft-tissue window automatically suppresses values that represent the lung tissue. As this window suppress most of the anatomy from the lung it can be used in lung region segmentation. Similarly, Lung Window images the lung anatomy where texture is highlighted better, as shown in Fig-2.

Windowing by software provides means by which we can manipulate the DICOM data to emphasize certain values. As mentioned earlier, in order to achieve a certain view (mediastinum, lung, etc.) there are three phases: first prospective reconstruction, second retrospective reconstruction and third is windowing using a software. The first two phases creates images from the raw data and the last phase takes the image created by the first two and reconstructs the different views from it. Changing the window setting merely in a DICOM data does not have the same outcome on the image as does with the raw data (as shown in **Fig-5**) because raw data include all measurements obtained from the detector array. When a reconstruction algorithm is used on a raw data it has the option of choosing among various attenuation values depending on the view type. In raw data there are various attenuation values for a point. So the algorithm uses the most appropriate value that will represent the view.

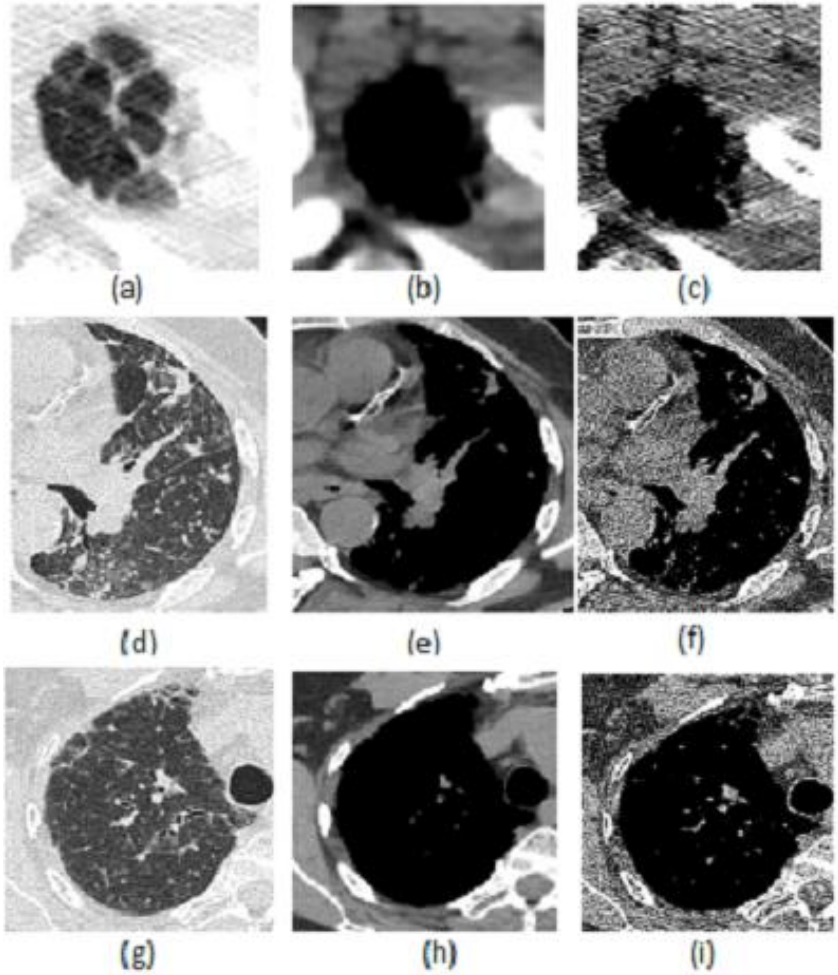

Fig 5: Cropped CT images showing the variation for different window settings- (a), (d), (g), represents the lung window. (b), (e) and (h), represents the mediastinum window. (c), (f) and (i), represents the software induced mediastinum window on lung windowed images.

The creation of mediastinum window image from lung window DICOM data by changing the window width/centre is referred to as swMW (software induced MW) images in this paper. The mediastinum window DICOM data created by prospective reconstruction is refer to as MW (mediastinum window) images and lung window DICOM data created also by prospective reconstruction is refer to as by LW (lung window) images.

II. RESEARCH METHODOLOGY

Dataset used:

The dataset used is a part of internal dataset of CT images collected from NABL (National Accreditation Board for Testing and Calibration) radiological laboratory. The dataset consists of variety of lung diseases which exhibit different texture patterns. To name a few, it consists of texture pattern like ground glass opacity, consolidation, emphysema, fibrosis, nodules and healthy lung. The images are in DICOM format, of resolution 512×512. The database consists of CT scans from 67 patients with abnormalities in it, each CT scan consists of two sets of images one set containing Mediastinum window (350-400 images) and one set containing lung window (350-400 images) images. Number of images for a single patient depends on patient anatomy. All of these scans are taken with hold breathing so there are very less anatomical changes due to breathing.

Segmentation Methods used:

Thresholding: Lung segmentation using pixel value intensity thresholding is a very computationally efficient method and produces acceptable results [1, 4, 10] in most of the instances. Here, a fully automated lung segmentation method was developed, which segments image in axial view and processes them sequentially. Pre-processing is done on each image before segmentation by threshold. In the pre-processing stage only lung window images are processed as processing the mediastinum view image have little impact on the segmentation results. This is because the level of background noise in mediastinum view is much less. To remove background noise from the lung view images, the image is convolved with a Gaussian kernel (radius of 1.90). This pre-processing step is equivalent of passing the image through a low pass filter.

An iterative thresholding method is proposed to segment the image.

Step 1: Scan the image to get the maximum V_{max} value and the minimum V_{min} value of gray in the image.
Step 2: Calculate the initial threshold

$$T = (V_{max} + V_{min})/2 \quad (3)$$

Step 3: Segment the image using *T*. This will produce two set of pixels: *F* (foreground) and *B* (background), that is one containing pixels whose gray values are greater than T and the other set containing pixels whose gray value are less than *T*.
Step 4: Compute μ_1 and μ_2, which is average pixel value of *F* and *B*.
Step 5: Calculate a new threshold value

$$T = (\mu_1 + \mu_2)/2 \quad (4)$$

and segment the image with new threshold,
Step 6: Repeat from 3 to 5 until the value of *T* stabilizes, i.e $T_{old} - T_{new} < \varepsilon$.
Step 7: Finally, morphological operators open and close are used to remove any background artefacts and to smooth the segmented image edges and fill any gap in the interior of the lung region.

Clustering: Clustering is grouping a set of pixel, such that, pixels belonging to a cluster are similar for that cluster. This similarity may be pixel intensity, pixels belonging to a certain shape and size or any other feature. In FCM the number of cluster to be formed is prior information [14]. Amongst many clustering techniques available, FCM is used extensively [5]. In FCM fuzzy weights are determined by reciprocal distance and the goal is to reduce the total weighted mean square error. Minimization of the objective function is given by:

$$J_m = \sum_{i=1}^{N}\sum_{j=1}^{C} \mu_{ij}^{m} \|x_i - c_j\|^2 \quad (5)$$

Where *m* is any real number greater than 1, x_i is the i^{th} pixel in a set of *N* pixels, c_j is the centre of the cluster, μ_{ij} is the degree of membership of a pixel x_i in a cluster *j*. An iterative optimization of the objective function is done for fuzzy partitioning and an update of membership μ_{ij} and cluster centre c_j is carried out by:

$$\mu_{ij} = 1/\sum_{i=1}^{c} \left(\frac{\|x_i - c_j\|}{\|x_i - c_k\|}\right)^{2/m-1}, \quad (6)$$

$$c_j = \sum_{i=1}^{N} \mu_{ij}^{m} . x_i \Big/ \sum_{i=1}^{N} \mu_{ij}^{m} . \quad (7)$$

This iteration will stop when $max_{ij}\left\{\left|\mu_{ij}^{(k+1)} - \mu_{ij}^{(k)}\right|\right\} < \varepsilon$, termination condition ε is between 0 and 1, *k* is the iteration step.

Segmentation validation: Sorensen-Dice coefficient or F_1 score is used to evaluate the segmentation accuracy. F_1 score measures the overlap of two segmentations: one being produced by an algorithm and another being the reference image (ground truth) The F_1 metric is a normalised metric and its value lies between 0(zero): no overlap and 1(one): total overlap. F_1 score is defined as follows:

$$F_1 Score = 2|I_{GT} \cap I_{seg}|/|I_{GT}| + |I_{seg}| \quad (8)$$

Where I_{GT} is the ground truth segmentation and I_{seg} is the segmented image performed by any algorithm.

III. RESULTS

To compare the segmented lung regions by the algorithm, a reference set of lung regions are required, known as masks. To create a reference mask, radiologists manually create lung masks that appropriately describe the lung region. The process of creating masks of lung region is a time consuming process since it takes on average 2-minutes to mark the lung region on an image. There are around 350-400 images per CT scan. Taking into account the voluminous time in masking the lung region and the fact that most of the images do not have much abnormality, we take help of automated region selection tool [6]. Thus radiologists improve upon selected images, which help improving accuracy and overall diagnosis time.

Implementation:

Fig-6 displays the results of segmentation for each of the windows from the dataset, by both implemented algorithms.

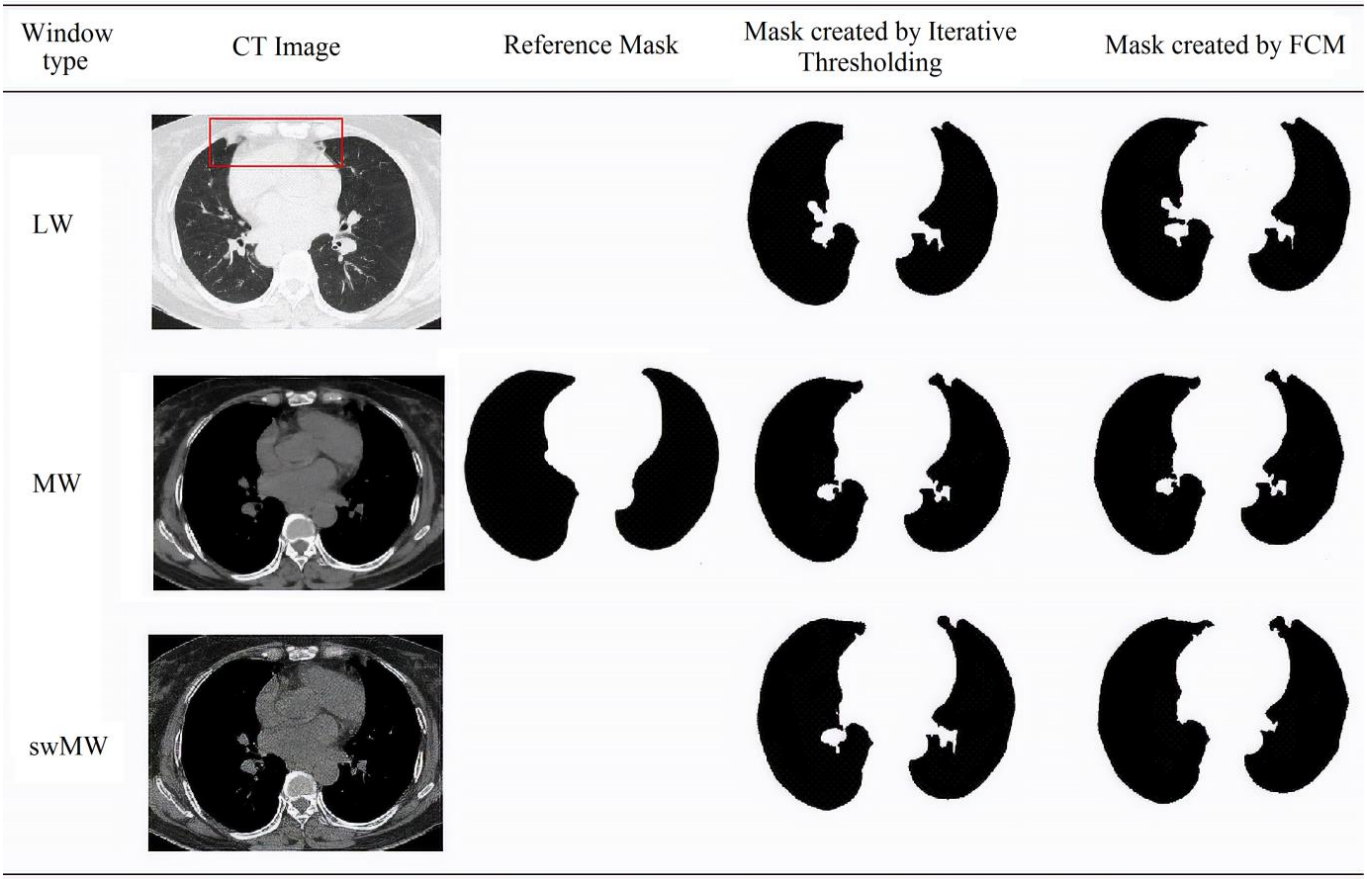

Fig 6: Segmentation of images from different window setting, Column titled CT image shows the images in different settings, segmenting peripheral abnormality (in red box). MW and swMW produces binary masks close to visual resemblance with the reference mask than LW.

To show the variation of segmentation accuracy when using MW images, LW images and swMW images F_1score is used. Since a single CT scan contain 350-400 images in a certain view and there are 67 such scans, so an average F_1score for the whole scan is reported instead of individual score. Two segmentation algorithm are used and there outcomes are stated below.

Thresholding- The F_1scores when thresholding algorithm is used on MW images, LW images and swMW images are given in **Fig-7**.

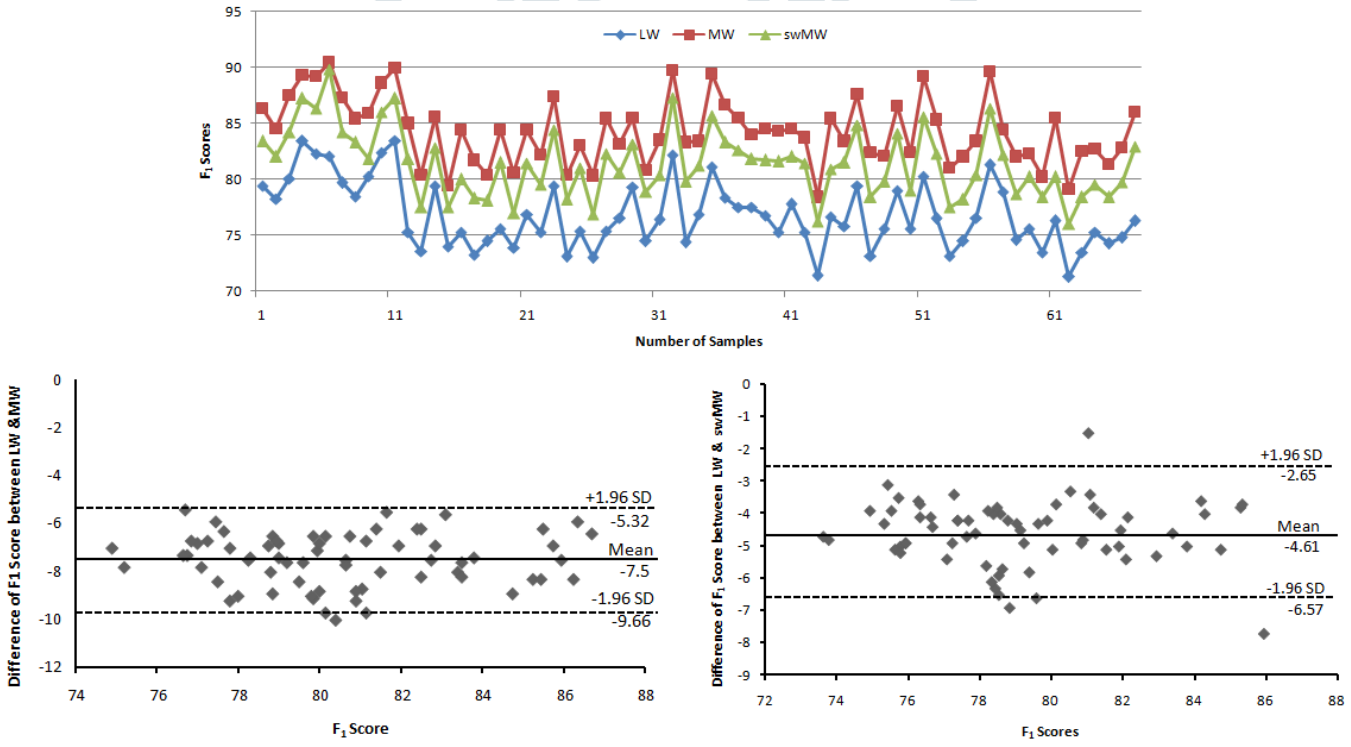

Fig 7: a)F_1scores using Thresholding algorithm b)Bland Altman plot between LW and MW c)Bland Altman plot between LW and swMW

The F_1scores of MW images are greater than that of both swMW images and LW images and, as evident from the figure, swMW images F_1score is greater than LW images. The segmentation of lung region by both MW and swMW images can replace the more prevalent LW images, as the agreement in the bland Altman plot is more than 95% for both.

Clustering: Another segmentation algorithm used to segment the lung region is FCM. The F_1scores for various image types are given in **Fig-8**. As evident from the F_1scores of MW images have values greater than that of LW images. The F_1score of swMW images also have scores higher than LW images. The agreement of bland Altman plot is more than 95% for both MW images and swMW images against the LW images.

IV. CONCLUSION

Images used for segmentation of the lung region are mostly in LW. Other windows like MW can produce better segmentation results, where emphasis is on mediastinum region. The mediastinum emphasis makes the lung region less anatomically detailed which helps in segmenting out the lung portion. MW is also resistant to some degree of opacity caused due to diseases. It is shown that MW images have higher segmentation accuracy with respect to LW images, while employing two different segmentation algorithm. If only LW images are available then changing the window width/centre to emphasis the mediastinum can produce segmentation results which are better than the LW images. Further, the accuracy of segmentation from MW images are higher than the software induced MW images (i.e. swMW), since MW images are created by using specific reconstruction algorithm on the raw data. Thus, while binary masks created on MW or swMW can both be used on the LW images, MW images are more preferable to have a better lung region segmentation. It has also been observed for other data sets (not used in this work) that MW images may have a different slice thickness. In that case a 3D mask can be generated using the MW images and use it to segment the LW images.

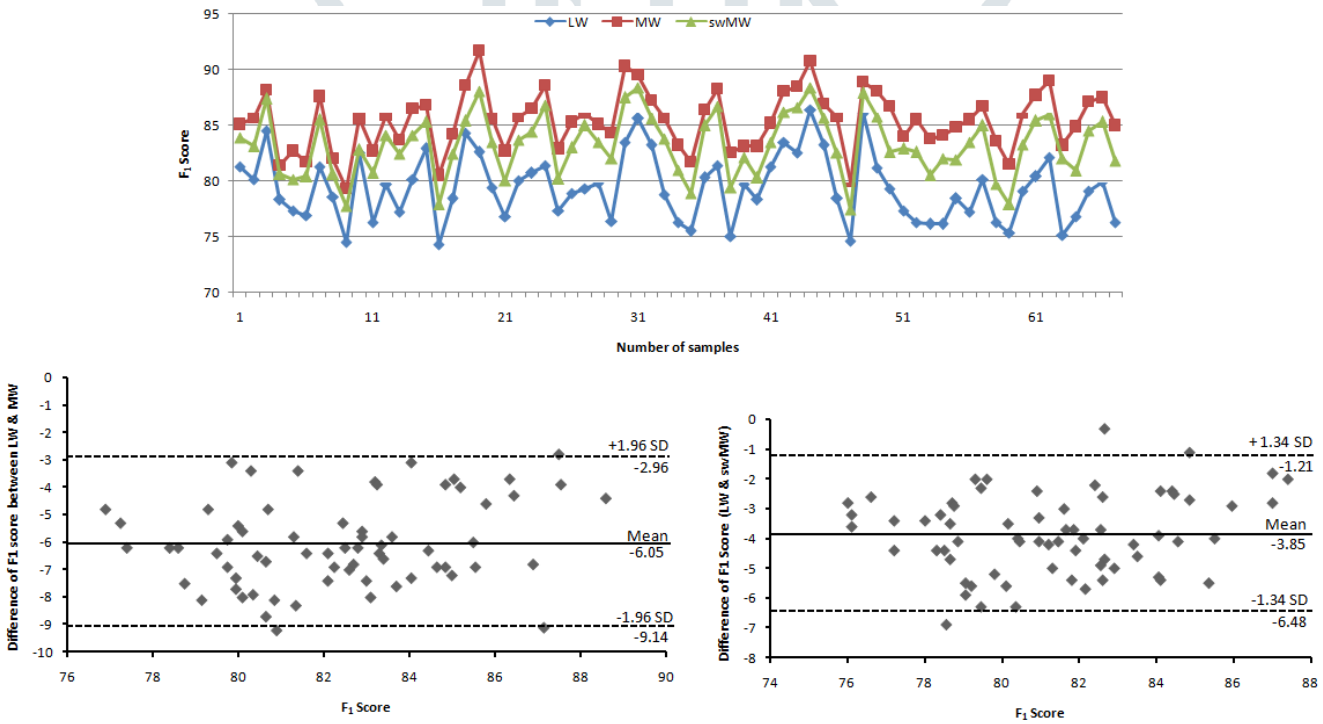

Fig 8: a)F_1 scores using FCM algorithm b)Bland altman plot showing agreement between LW and MW c)Bland altman plot between LW and swMW

V. ACKNOWLEDGMENT

We would like to thank NABL accredited Ayursundara Pvt. Healthcare Ltd., Guwahati, for their continuous support in this work by providing data needed for this study and help from there radiologists.

REFERENCES

[1] Ali, A.M., Farag, A.A. 2008. Automatic Lung Segmentation of Volumetric Low-Dose CT Scans Using Graph Cuts. Advances in Visual Computing, ISVC 2008. Lecture Notes in Computer Science, Springer, 5358: 258-267.

[2] Barnes, J. E. 1992. Characteristics and control of contrast in CT. Radio Graphics, 12(4): 825-837.

[3] Dai, S., Lua, K., Donga, J., et al. 2015. A novel approach of lung segmentation on chest CT images using graph cuts., 168: 799-807.

[4] Dawoud, 2011. Lung segmentation in chest radiographs by fusing shape information in iterative thresholding. IET Comput. Vision, 5(3): 185–190.
[5] Deen K. J. et al. XXX. Fuzzy-C-Means Clustering Based Segmentation and CNN-Classification for Accurate Segmentation of Lung Nodules. Asian Pacific Journal of Cancer Prevention, 18(7):1869-1874.
[6] GNU Image Manipulation Program (GIMP).https://www.gimp.org/, Accessed on 25.11.2018.
[7] Hofer, M. 2011. CT Teaching Manual: A Systematic Approach to CT Reading. Pub. Thieme, Edition 4, 2011.
[8] Hu, S., Hoffman, E.A., Reinhardt, J.M. 2001. Automatic lung segmentation for accurate quantitation of volumetric X-ray CT images. IEEE Trans Med Imaging, 20(6): 490–498.
[9] Jacobs, C. et al. 2014. Automatic detection of subsolid pulmonary nodules in thoracic computed tomography images. Med. Image Anal., 18: 374–384.
[10] Leader, J. K., Zheng, B., Rogers, R. M., et al. 2003. Automated Lung Segmentation in X-Ray Computed Tomography: Development and evaluation of a heuristic threshold-based scheme. Academic Radiology, 10(11): 1224-1236.
[11] Mansoor, A., Bagci, U., Xu, Z., Foster, B., Olivier, et al. 2014. A generic approach to pathological lung segmentation. IEEE Trans. on Medical Imaging, 33(12): 2293–2310.
[12] Mansoor, A., Bagci, U., Xu, Z., et al. 2015. Segmentation and image analysis of abnormal lungs at CT: current approaches, challenges, and future trends. Radio Graphics, 35(4): 1056–1076.
[13] Messay, T., Hardie R. C. and Rogers, S. K. 2010. A new computationally efficient CAD system for pulmonary nodule detection in CT imagery. Med. Image Anal., 14: 390–406.
[14] Nie, S., Li, L., Wang, Y., et al. 2012. A segmentation method for sub-solid pulmonary nodules based on fuzzy c-means clustering. Proceeding of IEEE 5th International Conference on BioMedical Engineering and Informatics, 169-172.
[15] Shojaii, R. and Alirezaie, J., Babyn, P. 2005. Automatic lung segmentation in CT images using watershed transform. IEEE International Conference on Image Processing, 2: II-1270.
[16] Xiaojiao X., Juanjuan, Z., Qiang Y., et al. 2018. An Automated Segmentation Method for Lung Parenchyma Image Sequences Based on Fractal Geometry and Convex Hull Algorithm. Applied Sciences, 8: 832.
[17] Zhenghao, S., Jiejue, M., Minghua Z., et al. 2016. Many Is Better Than One: An Integration of Multiple Simple Strategies for Accurate Lung Segmentation in CT Images. BioMed Research International, Article ID 1480423.